Atomic Nucleus as a Chaotic System

V. Zelevinsky

National Superconducting Cyclotron Laboratory and Department of Physics and Astronomy, Michigan State University, East Lansing, Michigan 48824-1321 USA

Abstract.

Many-body quantum chaos turns out to be a driving force of many important phenomena in nuclear structure and nuclear reactions. A review of "chaotic" physics and its manifestations, selected mostly by a personal interest, is presented.

1 "Regular" and "Chaotic" Dynamics

A standard explanation of nuclear structure starts [1] with the *independent quasi-particle* picture of fermions in a self-consistent *mean field*. The next step is related to the *many-body* states of such a system. The mean field determines the shape of the system, shell structure of the quasiparticle spectrum, magic numbers and in some cases predicts the main properties of low-lying states. The independent particle model cannot define the ground state of a system with more than one quasiparticles (quasiholes) with respect to the magic core. Here many opportunities for *angular momentum coupling* produce degenerate states. Finally, the *residual interaction* between the quasiparticles lifts the degeneracies and converts Fermi-gas into *Fermi-liquid*.

The founders of the shell model [2] assumed that there is an attractive *pairing* which prefers (for identical particles) pairs with total angular momentum $L = 0$ of the pair. There are many signatures of such pairing in nuclear dynamics [3, 4] which are kindred to superfluidity or superconductivity. It is usually assumed that just because of pairing all *even-even* nuclei have the ground state quantum numbers $J_0^\pi = 0^+$. Another important part of the effective residual forces is the *multipole-multipole*, mainly quadrupole, interaction [1, 4]. Different components of the residual interaction generate such features as shape vibrations and giant resonances of various types, alpha-correlations in light nuclei

and *quasideuteron* correlations. The latter are thought to be responsible for the isoscalar character of ground states of light *odd-odd* nuclei which can be represented by the deuteron-like pair in the $JT = 10$ state on top of the even-even core. In heavier odd-odd nuclei the isovector pairing prevails, and the ground state quantum numbers become $J_0T_0 = 01$; in all cases the selected combinations of J_0 and T_0 satisfy $(-)^{J_0+T_0} = -1$. All those forces are responsible for the *regular* features of nuclear dynamics. They create different sorts of elementary excitations; states with certain numbers of such excitons we can call "*simple*". However, the description in terms of independent simple excitations is approximate. The residual forces contain also many *incoherent* amplitudes of collision-like processes. These processes smear the ground state distribution of quasiparticles generating an analog of *temperature* [5, 6].

The many-body *level density* of a system of independent excitons grows with energy exponentially by pure combinatorial reasons. As soon as the residual interaction between the excitons becomes comparable with energy spacings we come to *mixing* of simple states. Actual stationary states are very complicated combinations of quasiparticle configurations. Neutron resonances in heavy nuclei are long-lived, practically stationary, states of a *compound nucleus* which are superpositions of approximately 10^6 independent shell model states. The giant resonances earlier considered as simple harmonic vibrations are getting fragmented over many eigenstates in the interval of the *spreading width*. The situation is complicated even more by the possible decay into continuum.

In the region of high level density it is impossible and meaningless to try to predict the properties of individual states. A small change in the parameters of the Hamiltonian will make unpredictable *local* variations in phases and amplitudes of individual components of a wave function. However the *global* features of the spectrum and observables are stable and can be studied by statistical methods. This is absolutely necessary for understanding the mechanism of various nuclear reactions.

On the other hand, characteristics of spectra and eigenstates turn out to carry important physical information. At this microscopic scale we deal with *quantum chaos* that reflects the deepest properties of dynamics related to symmetries and conservation laws. In the extreme limit these characteristics correspond to averaging over all Hamiltonians of a certain class, the next step after averaging over microstates for a given Hamiltonian performed in thermal Gibbs ensembles. This limit can be described by *random matrix theory* (RMT). Our goal below is to bridge the gap between local quantum chaos and global properties of strongly interacting quantum many-body systems, such as atomic nuclei. Many aspects of our discussion can be applied to other objects as complex atoms and molecules, clusters and grains of condensed matter, atoms in traps, solid state microdevices and prototypes of quantum computers. This area of physics is nowadays called *mesoscopic*. In the systems which are intermediate between macro- and micro-

world, we are lucky to be able to combine the statistical consideration with theoretical and experimental studying of individual quantum states.

2 Spectral Chaos

There are general regularities of spectra in complex systems that approach the limit of quantum chaos [7–9]. Originally they were considered as specific properties of *Gaussian ensembles* of random Hamiltonian matrices with the distribution functions of independent *uncorrelated* elements $H_{kl} = H_{lk}^*$,

$$P(H) = \mathrm{const}\, e^{-\mathrm{Tr}(H^2)/2a^2}. \tag{1}$$

For systems with time-reversal ($\mathcal{T}$-) invariance the basis can always be chosen as real, and the matrix H is real and symmetric (*Gaussian Orthogonal Ensemble*, GOE); it is clear that the function (1) is invariant under orthogonal transformations of the basis. Neither this distribution function nor its global predictions (for example, the *semi-circular* shape of the level density for a large dimension) are realistic. The studies of actual atomic and nuclear systems, as well as the interacting boson model, invariably give the distribution function of *many-body* matrix elements which depends on the representation and in the "normal" mean-field basis close to the exponential. The level density in the restricted shell model space is closer to the Gaussian [10] or binomial [11] rather than to the semicircle.

Moreover, the assumption of uncorrelated matrix elements is certainly wrong for the interaction of the *rank* (number of particles taking part in the acts of the residual interaction) significantly lower than the particle number. At normal nuclear or atomic density two-body processes (rank 2) are the most important ones. A given *two-body* process can take place for any spectator configuration of remaining particles so that the *many-body* matrix elements carry strong correlations. Apart from that, the exact (angular momentum) or nearly exact (parity, isospin) *conservation laws* are preserved even with chaotic interactions. The GOE ignores all such constraints except for energy conservation. Meanwhile, full chaos is not possible here since the Hilbert space is decomposed into nonmixing classes which are governed by the same Hamiltonian. Therefore the dynamics in different classes are expected to be correlated.

All these essential features of complicated many-body systems do not crucially influence the local spectroscopic properties governed by the strong mixing of close states. Starting with noninteracting particles in a mean field, we can consider the energy terms as functions of the overall interaction strength λ. At $\lambda = 0$ the levels correspond to various partitions of shell model space. At this point the dynamics are integrable and many levels for the same configuration but different spin-isospin quantum numbers JT are degenerate. Already at weak interaction the levels are mixed and the degeneracy is removed. For two closest neighbors at an initial distance ϵ the non-zero mixing matrix element V implies the increase

of the spacing to

$$s = \sqrt{\epsilon^2 + |V|^2}. \tag{2}$$

For an ensemble of multiple crossings in a $\mathcal{T}$-invariant system we consider ϵ and real V as random parameters with a distribution function $P(\epsilon, V)$. Introducing polar coordinates in the (ϵ, V)-plane, we have the spacing distribution function

$$P(s) = \int d\epsilon \, dV \, \delta(s - \sqrt{\epsilon^2 + V^2}) P(\epsilon, V) = s \int d\phi P(s \cos\phi, s \sin\phi). \tag{3}$$

Thus, at small spacings s, the levels *repel linearly* if the probability $P(0,0)$ is not singular. The singular behavior like $P(s) \sim s \ln(1/s)$ can occur, for example, in sharply cut band matrices [12].

In realistic many-body systems (Figure 1) the linear repulsion regime starts at a sufficiently high level density already at a relatively weak interaction, $\lambda \approx 0.2$. Using the scaled spacing variable, $s \rightarrow s/D$, where D is an average local spacing, $P(s)$ grows linearly at $s \rightarrow 0$, reaches its maximum near $s \approx 1$, and then goes down. The *Wigner surmise*

$$P_W(s) = \frac{\pi s}{2} e^{-(\pi/4)s^2} \tag{4}$$

approximates very well the GOE result. This is valid only for *pure sequences* of levels with identical exact quantum numbers. A superposition of sequences from different symmetry classes rapidly comes [13] to the Poisson distribution $P(s) = \exp(-s)$ with a maximum at $s \rightarrow 0$ that was discussed for nuclear spectra as early as in 1939 [14]. An interesting yet unsolved problem is related to the transition scenario from the Poisson case to the chaotic Wigner case induced by a perturbation that destroys symmetry and mixes unperturbed states. This question is crucial for the development of quantum computing where the elementary
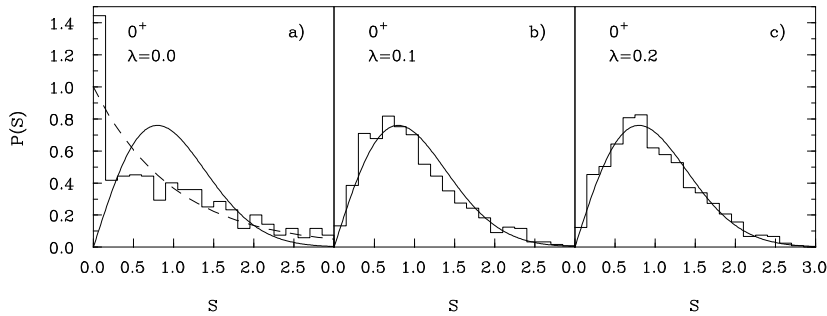

Figure 1. The nearest level spacing distribution for $J^\pi T = 0^+ 0$ states in the sd-shell model of ^{28}Si as a function of the overall strength of residual interactions, histogram; Wigner surmise, solid line; Poisson distribution, dashed line.

units (*qubits*) should interact in order to process the signal but weakly enough in order to keep the coherence of entangled states.

In the case of the violation of $\mathcal{T}$-invariance, the matrix elements are in general complex, and the extreme chaos should be described by the Gaussian Unitary Ensemble. In this case the level crossing would require the simultaneous vanishing of ReV and ImV, and instead of (3) we arrive at the quadratic repulsion, $P(s) \sim s^2$, at small s. This argument was used for a search of $\mathcal{T}$-violation in nuclear forces [15]. The situation is unusual: we are looking for the violation of fundamental symmetries via the finest details of complex spectra. The averaging which supposedly gets rid of all specificity of the system clears the way to basic laws of nature. Regrettably, the available statistics are too poor to make this search successful. Another limitation comes because all excited states are *quasistationary* so that their widths Γ, or energy uncertainty, change the spectral statistics at $s \leq \Gamma$ without any dynamic $\mathcal{T}$-violation.

Chaotic mixing makes the typical energy spectrum more rigid (an *aperiodic crystal* of levels). There are convenient measures of *spectral rigidity*, such as

$$\Delta(L) = \langle \min_{A,B} \int_x^{x+L} \frac{d\epsilon}{L} [\mathcal{N}(E) - AE - B]^2 \rangle_x. \tag{5}$$

Here $\mathcal{N}(E)$ is the cumulative number of unfolded (measured in units of the local spacing D) energy levels, and $\Delta(L)$ gives the deviation of this number from the best straight line fit averaged over overlapping segments of unfolded length L. For Poisson level statistics, $\Delta(L) = L/15$ grows linearly with the length L while in the chaotic case with a rigid level ladder, $\Delta(L)$ shows only a slow logarithmic growth. In a large-scale shell model diagonalization one can confirm [16] chaotic behavior of spectral rigidity up to very large $L \approx 2500$.

One can use spectral statistics in the analysis of mixed spectra. For example, thermal neutrons reveal well known narrow *resonances* in scattering off heavy nuclei. This is a typical mesoscopic region where one can study individual quantum states of a high degree of complexity. The strong resonances correspond to *s*-wave neutrons and, for an even-even target, have quantum numbers $J^\pi = 0^+$. But for odd-A targets with the ground state half-integer spin J_0 an *s*-wave resonance may have $J = J_0 \pm 1/2$. The spin value remains undetermined in experiments without polarization observables. However, the spectral statistics are aware of the mixed character of the level sequence and help determine the fraction of two possible spins J. The number of subsequences would be even larger if the K-quantum number, the total spin projection along the symmetry axis of a deformed nucleus, would still be conserved at excitation energy of neutron resonances. Thus, for the important case of ^{235}U with $J_0^\pi = 7/2^-$ the ground state has $K_0 = J_0 = 7/2$. The *s*-wave neutron resonance with $J = 3$ can have only $K = 3$ but for $J = 4$ two values, $K = 3$ and $K = 4$, are allowed so that the spectrum may contain three subsequences. The question of K-conservation is

still a subject of experimental and theoretical discussion [17].

Many authors studied spectra in various nuclear models and with real data. In spite of some deviations, especially at low energies, the nuclei seem to reveal a general agreement with the RMT at a rather weak interaction strength. Spectral statistics are insensitive to the details of dynamics and do not require the original assumptions of the RMT to be fulfilled. The local spectra of complex systems are close to universality determined by the most general symmetry properties.

3 Complexity

In RMT all stationary states are equally complex in almost all representations. Let us take an arbitrary basis $|k\rangle$ and express the exact eigenstates $|\alpha\rangle$ as superpositions

$$|\alpha\rangle = \sum_k C_k^\alpha |k\rangle. \tag{6}$$

The amplitudes C_k^α form a unitary (orthogonal for the $\mathcal{T}$-invariant case) matrix. If we loosely define N_α as a number of *principal* components, i.e. those carrying the lion's share of the total normalization,

$$\sum_k w_k^\alpha = 1, \quad w_k^\alpha \equiv |C_k^\alpha|^2, \tag{7}$$

we expect that the typical value of the weight of a principal component is $\overline{w_k^\alpha} \approx 1/N_\alpha$. We can use the number N_α to quantify the *degree of complexity* of the eigenstate $|\alpha\rangle$ *with respect to a given basis* $|k\rangle$.

In Gaussian ensembles N_α is the same for all states and coincides with the matrix dimension N. Indeed, in the GOE we have the joint probability distribution of components of any eigenstate which is invariant under orthogonal transformations and reflects only the normalization requirement,

$$P(\{C^\alpha\}) = \delta(\sum (C^\alpha)^2 - 1); \tag{8}$$

typical eigenvectors are uniformly spread over the surface of the N-dimensional sphere. This leads to the distribution function of a given component

$$P(C_k^\alpha) = \mathrm{const}[1 - (C_k^\alpha)^2]^{(N-3)/2}, \tag{9}$$

which is equivalent to the Gaussian distribution for large N,

$$P(C_k^\alpha) = \sqrt{\frac{N}{2\pi}} e^{-(N/2)(C_k^\alpha)^2}, \tag{10}$$

with the mean square value $1/N$ as expected.

With the Gaussian distribution of the components, the weights are distributed according to *Porter-Thomas* (PT),

$$P(w) = \frac{1}{\sqrt{2\pi\overline{w}w}} e^{-w/2\overline{w}}, \quad \overline{w} = \frac{1}{N}. \tag{11}$$

It is well known that the reduced neutron widths of neutron resonances indeed are distributed close to eq. (11). The neutron decay is the physical tool implementing the analysis of the wave function of a quasistationary state by singling out a component corresponding to the slow neutron in the continuum and the target nucleus in its ground state. This is one typical component and we expect that its distribution function will be generic one. We speak here about *reduced* widths with the threshold energy dependence ($\sim \sqrt{E}$ for s-wave neutrons) taken out; this dependence comes from the phase space restrictions rather than from the intrinsic matrix elements. This is similar to the level unfolding used in Section 1: we need to separate a global secular behavior from local properties. Since the complexity is basis-dependent we need to select a basis for comparing various wave functions. A natural choice for a many-body system is given by the *mean field* that is what remains after averaging out incoherent collision-like processes. This choice accomplishes the above mentioned separation. Actually, the mean field equations can be *derived* from the assumption that intermediate states in the nonlinear operator equations of motion are chaotic and have random phases [18]. Other choices of the basis can provide additional information.

The same PT distribution is expected to be valid for the strengths of specific operators, for example for a multipole transition from the ground state to a chaotic state with corresponding quantum numbers. The assumptions of the Wigner nearest level spacing distribution (4) and the PT distribution of strengths serve as a foundation of powerful statistical methods used by experimentalists [19] in order to recover the missing strength hidden in fine structure levels which are invisible in experiments with a relatively poor resolution.

Starting with a reference basis $|k\rangle$ of noninteracting quasiparticles and switching on the residual interaction, multiple avoiding crossings supply the wave functions $|\alpha\rangle$ with new components C_k^α. A convenient measure of the *delocalization* of the eigenstate $|\alpha\rangle$ in the given basis is *Shannon (information) entropy*

$$I_\alpha = -\sum_k w_k^\alpha \ln w_k^\alpha. \tag{12}$$

The starting ($\lambda = 0$) entropy I_k vanishes as for any wave function in its own basis. As λ grows, so does information entropy. For a state uniformly mixed among all basis states, all weights $w = 1/N$, and information entropy reaches its maximum $\ln N$. This wave function is fully delocalized, its delocalization length defined as $N_\alpha = \exp(I_\alpha)$ equals the space dimension. However, even

with the complete mixing, the orthogonality conditions do not allow all states to have $N_\alpha \approx N$. The fluctuations imminent to the GOE reduce the average value of N_α to $0.48\,N$.

The most important feature observed in shell model calculations is a smooth dependence of I_α on excitation energy. In the same narrow energy window the initial basis can place nearby the states of a very different nature. In the mixing process their entropies could remain different. Instead the adjacent states "look the same" [20]. For a sufficient interaction strength, they are equilibrated and entropies are equalized around the same value of λ that corresponds to the onset of the chaotic spectral statistics (the function $P(s)$ and N_α turn out to be strongly correlated [21]). The values of I_α still continue to grow with λ even beyond this equilibration, approaching the GOE value at high level density.

We mentioned earlier that the number N_α, as a measure of a number of principal components of the wave function, determines typical weights of components and probabilities of processes. But it does not take into account relative *phases* of the components and, strictly speaking, reflects delocalization rather than chaoticity. *Collective* states, being *coherent* combinations of many simple excitations, can have relatively large entropy. However, at high level density the collective states as giant resonances are mixed with complicated states of the same symmetry acquiring the *spreading width*. In the end the exact eigenstates show only a fragmented excess of collective strength in this region. This reminds the phenomenon of *scars* known from one-body chaos [22]: a remnant of a collective mode marks the complicated states.

A more dangerous aspect is related to the evolution, or phase transitions of the mean field with excitation energy that would be better accounted for by changing the reference basis. In such cases information entropy in the fixed basis does not reflect properly the complexity of the state. Here it may be useful to look at *correlational* (von Neumann) entropy [23] defined through the response of a state $|\alpha\rangle$ to an external random perturbation. Let λ be a random parameter in the Hamiltonian. The energy terms $E_\alpha(\lambda)$ and the coefficients $C_k^\alpha(\lambda)$ in an *arbitrary* basis $|k\rangle$ are random quantities, and we can form a *density matrix* of a given state

$$\rho_{kk'}^\alpha = \overline{C_k^\alpha C_{k'}^{\alpha*}} \qquad (13)$$

where we average over the distribution function of the noise λ. This density matrix defines correlational entropy

$$S_\alpha = -\mathrm{Tr}(\rho^\alpha \ln \rho^\alpha) \qquad (14)$$

which is now basis-independent and contains information on phase relations. With fixed parameters λ, the density matrix ρ^α has one nonzero (equal to 1) eigenvalue which projects out the state $|\alpha\rangle$ whereas other eigenvalues vanish. This is a *pure* quantum state, entropy $S^\alpha = 0$, and $(\rho^\alpha)^2 = \rho^\alpha$. In the presence

of noise we deal with the *mixed* quantum state, and ρ^α acquires nonzero eigenvalues between 0 and 1; always $\mathrm{Tr}\,\rho^\alpha = 1$. In perturbation theory every new order brings in a new nonzero eigenvalue and increases entropy. This entropy is closer to statistical entropy of a system in the environment and in some cases the noise leads to a thermal equilibrium ensemble. S^α is sensitive to phase transitions in the system [24]. It is well known that the notion of entropy refers not to a specific quantity but rather to a family of concepts [23], and various members of this family can be useful in various circumstances. In particular, one can relate information entropy to thermodynamics and establish a new paradigm of statistical mechanics of finite quantum systems [5, 16, 25, 26].

4 Enhancement of Perturbations

Perhaps, the most practically important consequence of the chaotic mixing is the enhanced sensitivity to weak perturbations. The source of this enhancement can be seen in the N-*scaling* of the complexity [27]. Let us consider matrix elements of a simple, for example one-body, $\sim a^\dagger a$, operator $\hat{Q}$ between a chaotic state $|\alpha\rangle$ and a "simple" state $|k\rangle$,

$$\langle k|\hat{Q}|\alpha\rangle = \sum_{k'} C^\alpha_{k'} \langle k|\hat{Q}|k'\rangle. \tag{15}$$

The selection rules for the operator $a^\dagger a$ single out few initial states $|k'\rangle$ for a given final state $|k\rangle$. The effective factor ν coming from the presence of such states is determined by the geometric coupling of Slater determinants for the given shell model partition into a normalized state with given total spin. If the single-particle matrix elements of the operator $\hat{Q}$ can be estimated by their average value q, we come to

$$\langle k|\hat{Q}|\alpha\rangle \approx \frac{q\nu}{\sqrt{N_\alpha}}, \tag{16}$$

where N_α is a complexity of the state $|\alpha\rangle$. A very similar estimate can be obtained for the transition between two chaotic states of a similar degree of complexity N,

$$\langle \alpha|\hat{Q}|\beta\rangle = \sum_{kk'} C^{\alpha*}_k C^\beta_{k'} \langle k|\hat{Q}|k'\rangle. \tag{17}$$

Again here exist a tight correspondence between the states $|k\rangle$ and $|k'\rangle$. If the components of complex states are uncorrelated, we estimate the remaining sum as a random walk and again arrive at

$$\langle \alpha|\hat{Q}|\beta\rangle \approx \sqrt{N} \left(\frac{1}{\sqrt{N}}\right)^2 q\nu = \frac{q\nu}{\sqrt{N}}. \tag{18}$$

Thus, typical matrix elements including simple operators and complicated states are suppressed $\sim 1/\sqrt{N}$.

The perturbation $\hat{h}$ induces an admixture to the wave function,

$$|\Psi\rangle \rightarrow |\Psi'\rangle \approx |\Psi\rangle + \frac{\langle\Psi'|\hat{h}|\Psi\rangle}{\Delta E}, \qquad (19)$$

where ΔE is an unperturbed level spacing. Comparing the mixing of simple states with that in the chaotic region we see the interplay of two opposite trends: reduction, $\sim 1/\sqrt{N}$, of the mixing matrix element between complicated states, and, at the same time, increase of the level density and therefore decrease of the energy denominator ΔE. The mixing of adjacent states ($\Delta E \propto 1/N$) is expected to be *enhanced* $\sim \sqrt{N}$ compared to the mixing among single-particle excitations. This *statistical enhancement* of perturbations is another expression of quantum chaos. The brightest manifestation is seen in *parity ($\mathcal{P}$) violation*. $\mathcal{P}$-odd forces have their origin in fundamental electroweak interactions. Under normal circumstances, their effects are of the order of $10^{-(7-8)}$ as seen, for example, in large β-decay lifetimes. The experiments with polarized slow neutrons show a different picture. The cross sections for scattering of neutrons of left and right helicity differ because of $\mathcal{P}$- nonconservation. But, instead of being $\sim 10^{-7}$, this difference in some nuclei reaches 10% of the average cross section; the nuclei with the large effect were predicted theoretically [27]. $\mathcal{P}$-nonconservation mixes p- and s-wave neutron resonances, i.e. chaotic wave functions of complexity $N \sim 10^6$. The mixing operator is a $\mathcal{P}$-violating part of the mean field in a form of the anticommutator $[(\vec{\sigma} \cdot \mathbf{p}), \rho(\mathbf{r})]_+$. Our estimates predict the statistical enhancement of the order 10^3. Another factor comes from the *kinematic* enhancement: the asymmetry is proportional to the ratio of s- and p-neutron widths which, near threshold, is also of order 10^3.

If the statistical mechanism is correct, one should expect the random *sign* of the asymmetry which is indeed observed for nearly all cases. The notorious exception is ^{232}Th where all ten resonances with significant asymmetry have the same sign. The reason might be related [28] to the structure of this nucleus. If it has octupole deformation at energies near neutron threshold, the $\mathcal{P}$-doublets should exist. They can be mixed by the weak interaction together with Coriolis forces in the deformed rotating nucleus; being in a sense mirror reflections of each other they have fully correlated chaoticity. Hypothetical forces simultaneously violating $\mathcal{P}$- and $\mathcal{T}$-symmetries should be especially enhanced in such cases since their mixing does not require a mediator as Coriolis interaction.

Even more impressive manifestation of statistical enhancement is seen in *fission of heavy nuclei by polarized neutrons* [29]. Here the signature of $\mathcal{P}$-violation is the asymmetry $(\vec{\sigma} \cdot \mathbf{P}_f)$ of a fission fragment with respect to the direction of the primary neutron spin. Surprisingly, a small initial asymmetry of a single neutron helicity is transformed in an ordered motion of hundreds of nucleons. The observed asymmetry is on the level of 10^{-4} because here there is no

kinematic effect. The mixing of the resonances of opposite parity again works at the *hot* stage of a compound nucleus [27]. The fissioning nucleus is going through a pear-shaped configuration where the memory of $\mathcal{P}$-nonconservation is transformed into the asymmetry of fragment motion. The asymmetry is nearly independent of the final mass asymmetry or kinetic energy distribution - all those characteristics are decided on the *cold* stage of the process *after* the parity mixing has already occurred. Since at this point the original excitation energy is converted into deformation, there are only few open fission channels so that the final result is not averaged out.

5 Strength Function

The N-scaling is important for understanding the fragmentation of basis states $|k\rangle$ over eigenstates $|\alpha\rangle$. In the time-dependent formulation, this is seen as *damping* of an initial state. The time scale is set by the *spreading width* of the *strength function*

$$F_k(E) = \sum_\alpha w_k^\alpha \delta(E - E_\alpha) \equiv \langle k|\delta(E - \hat{H})|k\rangle. \tag{20}$$

The Fourier-component of the strength function,

$$f_k(t) = \int dE\, e^{-(i/\hbar)Et} F_k(E) \equiv \langle k|e^{-(i/\hbar)\hat{H}t}|k\rangle, \tag{21}$$

is the amplitude of *survival* of the original state $|k\rangle$. The centroid of the strength function,

$$\bar{E}_k = \int dE\, E F_k(E) = \langle k|\hat{H}|k\rangle, \tag{22}$$

is just a diagonal matrix element of the Hamiltonian, while the energy dispersion σ_k of the initial state is the second central moment,

$$\sigma_k^2 = \int dE\, (E - \bar{E}_k)^2 F_k(E) = \langle k|(H - \langle k|H|k\rangle)^2|k\rangle. \tag{23}$$

The strength function is normalized, $\int dE\, F_k(E) = 1$, whereas the sum over the basis states,

$$\rho(E) = \sum_k F_k(E) = \mathrm{Tr}\{\delta(E - \hat{H})\}, \tag{24}$$

is the total level density which justifies a frequently used name of the strength function as *local density of states.*

A preliminary knowledge about the strength functions of basic states can be acquired prior to the diagonalization of the matrix $\hat{H}$. Thus, the centroid is given

by eq. (22), and the dispersion (23) can be calculated as a sum of off-diagonal matrix elements,

$$\sigma_k^2 = \sum_{k' \neq k} |\langle k'|\hat{H}|k\rangle|^2. \tag{25}$$

When the shell model states $|k\rangle$ are JT-projected combinations of Slater determinants of the m-scheme, the quantity σ_k only weakly fluctuates within a given JT-class and can be approximated by a constant $\bar{\sigma}$. This is a result of *geometric chaoticity* of vector coupling of individual spins and isospins. An approximately constant value of σ_k leads one to an idea of a generic shape of the strength function for complex states of a given class. The formal calculation of the strength function proceeds as follows [1]. Let the matrix obtained by the elimination of the state $|k\rangle$ be diagonalized. This gives the set of the intermediate eigenstates $|\beta\rangle$ and their energies ϵ_β with the level density quite close to the full one (only one state was excluded). The excluded state $|k\rangle$ is coupled to the set $|\beta\rangle$ by the matrix elements $V_{k\beta}$ of residual interaction transformed to the new basis. The secular equation for exact energies E_α has the form

$$E_\alpha - \bar{E}_k - \sum_\beta \frac{|V_{k\beta}|^2}{E_\alpha - \epsilon_\beta} = 0. \tag{26}$$

If a nearly equidistant spectrum ϵ_β stretches far away on both sides of the centroid $\bar{E}_k$ with a mean spacing D and weakly fluctuating coupling strengths $|V_{k\beta}|^2$, eq. (26) predicts the Breit-Wigner (BW) shape of the strength function $F_k(E)$ with the *golden rule* spreading width

$$\Gamma_s = 2\pi \frac{\overline{|V_{k\beta}|^2}}{D}. \tag{27}$$

The width Γ_s indicates the *exponential decay*, $\sim \exp(-\Gamma_s t)$, of the initial nonstationary wave packet $|k\rangle$. These assumptions and related results can be called the *standard model* of the strength function.

   Due to the N-scaling, the spreading width (27) is a very stable characteristic of the many-body Hamiltonian. The density of states $1/D$ increases $\sim N$ while the matrix elements decrease $\sim 1/\sqrt{N}$. Therefore the quantities that depend strongly on excitation energy are eliminated, and the spreading width *saturates* as soon as the system is in the chaotic regime, on the level predetermined by the residual interaction. One of the examples is given by the *isobaric analog states* [30]. Their spreading widths associated with the mixing of the states of isospin $T_>$ with numerous complex states of smaller isospin $T_> - 1$ vary very little in the region of 50-100 keV for different nuclei, excitation energies, spins, parities and isospins (one can notice only gradual increase for heavier nuclei). The intrinsic widths of giant dipole resonances in heated nuclei apparently are also

saturated as a function of excitation energy in heavy ion reactions, although here the situation is more complicated both experimentally (effects of the entrance angular momentum) and theoretically (sensitivity to the nuclear shape which also fluctuates with temperature).

The BW shape of the strength function cannot be exact since it corresponds to the infinite energy dispersion (23) and precisely exponential decay. But for a relatively weak coupling to the environment and in all situations, where the wings of the strength are of minor significance, the standard model gives a good approximation. It becomes invalid [31] when the state is *coupled strongly* to the environment, and the spreading width Γ increases beyond the region δE where the coupling matrix elements and/or level density are approximately constant. The shape is getting closer to Gaussian [32, 33], and the spreading width can be estimated as $\Gamma \approx 2\bar{\sigma}$ in terms of the energy dispersion (23). The saturation of the spreading width still takes place but the dependence on the interaction strength λ changes from *quadratic* in the standard model (27) to *linear* in the strong coupling regime. This evolution can be parameterized by a simple interpolation

$$\Gamma(\lambda) = \frac{a\lambda^2}{1 + b\lambda} \tag{28}$$

where the parameters a and b can be found directly from the limits of weak and strong coupling. Eq. (28) describes very well the results of the exact shell model diagonalization [33].

The deviations from the standard model and BW shape of the strength function are amplified in the widths Γ_n of the *multiple giant resonances* [32]. The arguments based on the standard model predict $\Gamma_n/\Gamma_1 = n$ because of the Bose-factor of induced radiation in the matrix elements that couple an n-phonon state with the background. This agrees with the convolution of n single-phonon strength functions of BW shape. The observed widths of double giant dipole excitations are significantly narrower, $\Gamma_2/\Gamma_1 \approx 1.4 \div 1.5$. This is expected in the strong coupling regime when the spreading width has a linear dependence on coupling matrix elements and, consequently, on the Bose factor,

$$\Gamma_n = \sqrt{n}\,\Gamma_1. \tag{29}$$

Phenomenologically, it follows from the convolution of the two Gaussians when the widths are added in quadratures. Even if the system is in the intermediate regime between weak and strong coupling, the convolution amplifies the deviations from BW shape and, according to the central limit theorem, approaches the Gaussian case.

6 Exponential Convergence

The realistic shell model case is close to the strong coupling regime and Gaussian shape [33]. However, the remote wings fall off slower displaying the *exponential*

drop-off. This means that in the tails the strength function is exponentially small being proportional to the entire remaining strength,

$$F(E) = \text{const} \int_E^\infty dE' \, F(E') \quad \rightsquigarrow \quad F(E) \propto e^{-\text{const} \cdot E}. \tag{30}$$

The energy wings reflect the initial stage of the nonexponential decay of the survival amplitude (21) when $|f_k(t)|^2 \approx 1 - \sigma_k^2 t^2$. Moreover, this should be a generic property since the energy dispersion σ_k is almost constant.

Increasing the size of the matrix with new partitions, we invariably see, in agreement with the above arguments, that the energy eigenvalues monotonously converge to exact numbers the convergence being pure *exponential*. This property was checked both for random matrices and for realistic shell model cases [35]. This opens the way to huge shell model spaces by exact diagonalization of few progressively truncated matrices, still of a tractable dimension, with the following exponential extrapolation. Such a procedure was implemented for fp-shell nuclei [36]. It was found that the regime of the exponential convergence
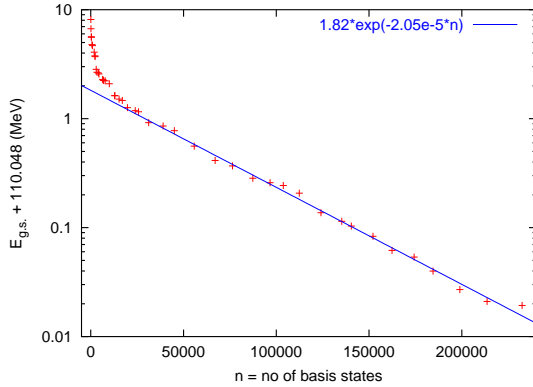
With exponentially small remote admixtures, the energy of a low-lying state can be derived in a good approximation by a reasonable *truncation* of the huge Hamiltonian matrix. Since the spreading width in the strong coupling regime $\Gamma \approx 2\bar{\sigma}$, we can start with a truncation on the level of $(3 \div 4)\bar{\sigma}$ from the original state. In order to not violate the shell model symmetry we need first to establish spectroscopic centroids of the partitions, and then include in the primary diagonalization all partitions (in their entirety) within a desired distance. Indeed, this approximate procedure [34] gives the energies in the limits of few hundred keV from the exact value. The approximate wave functions also have a large, $\sim 90\%$, overlap with the exact solution.

Figure 2. Shell model calculation of the ground state energy in ^{49}Cr and exponential fit as a function of the increasing dimension; notice the faster convergence at the initial stage (onset of chaos).

indeed starts at a truncation size of $(3 \div 4)\bar{\sigma}$, see Figure 2. The expectation values of observables can be also found with the exponential extrapolation although here one has to be careful taking into account the specific selection rules for different operators which can create a *non-compact* strength function with several maxima in different energy intervals.

The exponential convergence was observed in various physical problems involving spaces of a large dimension. The mathematical justification can be given with the help of the Lanczos algorithm which reduces the original matrix to a tridiagonal one where one should compare the asymptotics of diagonal and off-diagonal elements [35].

7 Ordered Spectra out of Chaos

We have already mentioned that conservation laws and the two-body nature of interaction introduce the correlations which are absent in the pure RMT. In a restricted orbital space there are few independent interaction parameters, namely reduced matrix elements $V_{Lt}(12; 34)$, where L and t are total spin and isospin of the pair, respectively. There are 63 such matrix elements in the sd-shell model space. These parameters, along with the single-particle energies, govern the dynamics in all JT-classes introducing correlations *between the classes*, a new element in theory of many-body quantum chaos. The simplest manifestation of such correlations is the presence of long rotational bands in nuclear spectra. There is an idea by Mottelson that even in a compound nucleus, where the typical states are chaotic, the strong preferential intraband transitions may exist. With strong mixing between adjacent states with the same quantum numbers, one would expect that a rotational state will emit γ-rays to many final states of another class creating a *turbulent* deexcitation flow. However, if the chaotic mixing in the different J-classes is similar, it may happen that the rotational state still has a strong overlap with its counterparts on the next step keeping an almost *laminary* pattern of few parallel deexcitation paths. Such *compound bands* were seen in shell model calculations but still remain to be seen in nature.

The ground state spins of all even-even nuclei are known to have $J^{\pi} = 0^+$ and the lowest possible isospin. This is traditionally thought [2] to follow from the strong attractive pairing. The unexpected results of ref. [37] made this conventional wisdom questionable. The shell model calculations with degenerate single-particle energies and *random* interaction matrix elements V_L lead to a high probability of the ground state spin $J_0 = 0$. This puzzle attracted attention of many authors who studied the problem in detail [38–41] and showed that the conclusion is insensitive to the specific properties of the random ensemble. Similar results are obtained for interacting bosons [42]. Unfortunately, many numerical simulations which show new aspects of the problem give no physical insight in what is going on. Below we briefly list different ideas, with their pluses and minuses.
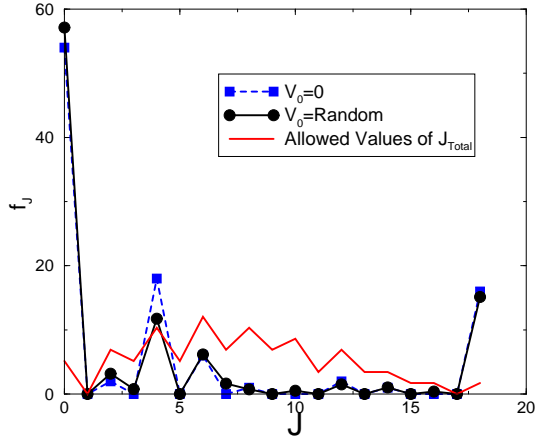
Figure 3. Fraction of ground states with spin J in the uniform ensemble of random two-body interactions for $A = 6$ particles on a $j = 15/2$ level, solid line; the same random ensemble without pairing, $V_0 \equiv 0$, dashed line; multiplicity $\mathcal{N}(J)$, thin line.

Multiplicity $\mathcal{N}(J)$ of states with spin J does not give any preference to $J = 0$. Using the standard idea of random coupling of individual spins, the result can be well approximated by

$$\mathcal{N}(J) \approx \text{const} \cdot (2J + 1)e^{-J(J+1)/2I}, \qquad (31)$$

where I is a spin-cutoff factor depending on available single-particle states. The maximum of multiplicity never comes to $J = 0$, see Figure 3.

A width $\sigma(J)$, *a second moment of the level density* $\rho_J(E)$, can be found by methods of statistical spectroscopy [43] being usually slightly greater for $J = 0$ than for $J = 2$. However this, in turn, requires its own physical explanation. Moreover, the excess of width $\sigma(0)$ is too small to create the observed predominance of $J_0 = 0$. In addition, high values of J have, as a rule, even larger widths.

Effective pairing correlations might appear as a result of averaging effects of random interactions. However, the preponderance of $J_0 = 0$ changes very little if the pairing component of the two-body interaction is set to zero in the ensemble, Figure 3. The ground state wave functions are far from those expected for developed pairing correlations; they are close [44, 45] to the chaotic RMT limit, eq. (9), see Figure 4. The shell model calculation in the sd-space with random interactions discovered [45] in some cases a slightly enhanced overlap of the ground states with the realistic paired states. This can be traced to the *off-diagonal* pairing matrix elements. In the second order their effect does not depend on sign and brings the states with the elements of pairing correlations down. In the model where those random off-diagonal elements are the only non-zero parts of the residual interactions, the probability of $J_0 = 0$ is higher than 90%.
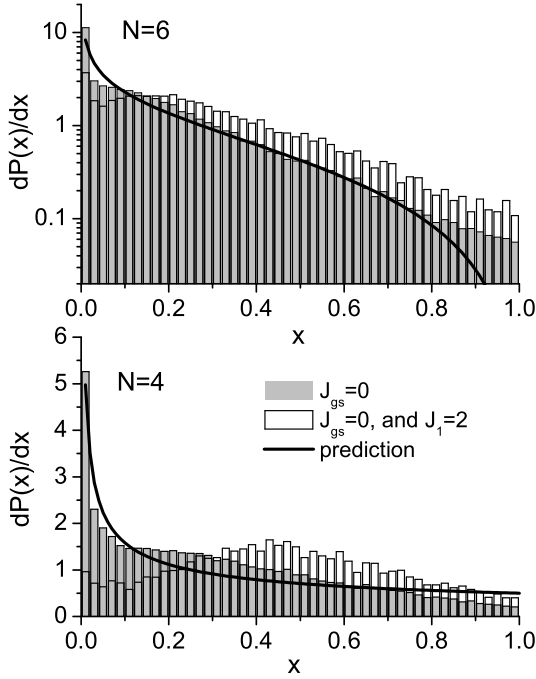
Figure 4. The distribution of overlaps $x = |\langle \tilde{0}|0\rangle|^2$ of the ground states $|0\rangle$ with $J_0 = 0$ for a Gaussian ensemble with the fully paired state $|\tilde{0}\rangle$ of seniority 0, for 4 (lower part) and 6 (upper part) particles, shaded histogram; the same for the additional constraint of the first excited state $J = 2$, open histogram (the excess is a measure of non-statistical effects); random matrix prediction, solid line.

Matrix elements V_L, taken alone (at a negative value), determine the ground state spin $J_0(V_L)$. The fraction of matrix elements leading to $J_0 = J$ can be taken [46] as a measure of total probability of this ground state spin. This observation is valid [47] in the rare cases when the quantum numbers, such as J and seniority, uniquely characterize the state so that the wave function is known and total energy is a *linear function* of V_L (even then the physical foundation of the result is still missing). This sampling of the corners of the parameter space is not sufficient in realistic cases requiring the diagonalization of the matrix [48].

Collective strength was claimed [37, 38] to be enhanced for the multipole transitions from the ground state with random interactions. This was a result of the maximizing the effect by the construction of a special transition operator for each copy of the ensemble. With the fixed multipole operator, the collectivity does not appear [45].

Time-reversal invariance is spontaneously broken in the ground state with

$J_0 \neq 0$ by a choice of the projection M. The rotation restores this invariance serving as a Goldstone mode. From this viewpoint, the state with $J = 0$ is singled out. This is not related to direct $\mathcal{T}$-violation [39]. The probabilities do not change after the $\mathcal{T}$-odd (imaginary) random interaction is explicitly introduced since the odd orders are averaged away.

A boson representation of fermionic pairs, $(a^\dagger a^\dagger)_{L\Lambda} \rightarrow b_{L\Lambda}$, reveals an effect [44] favorable for $J_0 = 0$. Such an approximation, the first term of a regular boson expansion, when the matrix elements V_L play the role of single-boson energies, works if the occupation of the shell is not very large. Then the ground state is a condensate of bosons b_L for the pair spin L with the strongest attractive V_L. For a single-j level, there are $k = j + 1/2$ even values of L allowed by Fermi-statistics. The probability for V_0 to be the most negative is $\sim 1/k$. Therefore, independently of multiplicity $\mathcal{N}(0)$, the probability of $J_0 = 0$ is greater than $1/k$. For the cases when the strongest attraction occurs for $L > 0$, the condensed bosons have another chance to couple to $J = 0$. The next terms of boson expansion contain the *boson pairing* which acts coherently and brings the states with $J = 0$ down, lifting the degeneracy of the condensate states and increasing the total probability for $J_0 = 0$. Still this mechanism is not sufficient for explaining the predominance of $J_0 = 0$ since the fraction $1/k$ decreases as the fermionic space grows.

The maximum spin ground state, a ferromagnetic case, has in many cases an enhanced probability as well [39, 44], in particular if one takes into account that its multiplicity is quite low (there is only one state with $J = J_{max}$ in a single-j case). This implies the crucial role of geometric effects.

The effective Hamiltonian after averaging the results of many realizations can depend [44] only on *constants of motion*, as particle number, spin and isospin (see similar arguments for quantum dots [49]). At small values of J and T, it should be an expansion of the form

$$\hat{H}_{eff} = H_{00} + H_{20}\mathbf{J}^2 + H_{02}\mathbf{T}^2 + H_{22}\mathbf{J}^2\mathbf{T}^2 + H_{40}\mathbf{J}^4 + \ldots \qquad (32)$$

If the series converges, in average we should have a "rotational band" with random moments of inertia in J and T. The results are determined by the sign of the moments of inertia. The area $H_{20} > 0$ determines the domain of $J_0 = 0$ (an *antiferromagnetic* case). The coefficients H_{pq} depend on the particle number A.

The idea of geometric chaoticity [44] helps in understanding physical reasons for the predominance of $J_0 = 0$ states. One can estimate the coefficients of the effective expansion (32) for Fermi-gas. Assume that in average the interaction does not create a significant mean field, and the equilibrium (thermodinamically favorable) distribution of the particles is the one that maximizes single-particle entropy under necessary constraints. Take a representative state with the maximum projection $M = J$. The equilibrium (in a single-j case) corresponds to the

occupancies

$$n_m = [\exp(\gamma m - \mu) + 1]^{-1}, \tag{33}$$

where the chemical potential μ and the effective magnetic field, or the cranking frequency around the symmetry axis, γ, are fixed by the requirements

$$\sum_m n_m = A, \quad \sum_m m n_m = M. \tag{34}$$

The statistical average of the microscopic Hamiltonian over the particle distribution (33) is

$$\langle \hat{H} \rangle \approx \sum_{L\Lambda} V_L \left(C_{mm'}^{L\Lambda} \right)^2 n_m n_{m'}, \tag{35}$$

where $C_{mm'}^{L\Lambda}$ are Clebsch-Gordan coefficients. Expressing the Lagrange multipliers in terms of A and J (no isospin in this model) we come to the effective form (32). In this approach $\langle \hat{H} \rangle$, and therefore the coefficients H_{pq}, are *linear* in V_L and, in the quadratic approximation to (32), we obtain the 50% probability of $J_0 = 0$, regardless of the multiplicity $\mathcal{N}(0)$. For $J \approx J_{max}$ the expansion (32) is invalid but a consideration is easy because the wave function is unique. Taking a correction for higher than quadratic terms (the series indeed converges rapidly) we obtain the prediction for the $J_0 = 0$ probability in qualitative agreement [44] with calculations for the ensemble of random interactions. Thus, correct estimates of probabilities for the ground state spin follow from a simple statistical approach. Details of geometry ignored in this approximation lead to the non-monotonous behavior. The probability for $J_0 = J_{max}$ gradually decreases for larger spaces.

The value of ground state energy predicted by eq. (35) with the occupation numbers (33) is clearly correlated with the actual value from the exact diagonalization [44]; a good agreement exists for J_{max} but for low spins there are still systematic deviations. In this simplest approach, possible mean field effects are neglected. Although in average the fields due to different components of random interactions cancel, the fluctuations are important. In a refined theory we need to take into account the effective deformation, specific for each copy of the ensemble, that splits single-particle levels. In a single-j model and in keeping with the statistical approximation (35), the deformed spectrum is given by

$$\epsilon_m = 2 \sum_{L\Lambda} V_L \sum_{m'} \left(C_{mm'}^{L\Lambda} \right)^2 n_{m'}, \tag{36}$$

which, after a self-consistent correction to n_m, introduces nonlinear correlations neglected in the oversimplified assumption (33). Using in the statistical approximation (35) instead of (33) the occupation numbers n_m from the actual wave
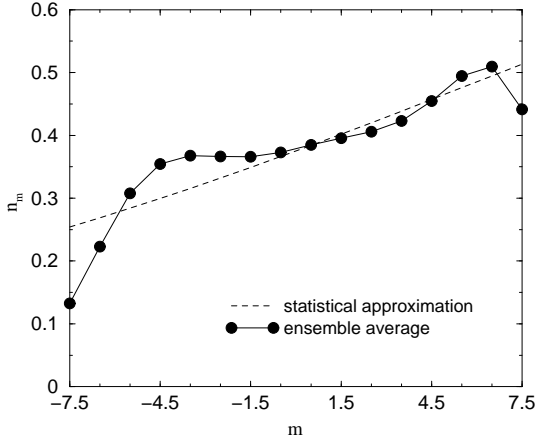
Figure 5. Average over the ensemble occupation numbers of the magnetic substates for 6 particles, $j = 15/2$, $J = M = 6$, given by the statistical approximation, eq. (33), dashed line, and from actual data, solid line.

function, Figure 5, we considerably improve the relation between the model and numerical experiments. The mean field also explains similar regularities observed for randomly interacting bosons [41].

New effects are brought in by isospin [48]. The lowest isospin value is always preferred for the ground state, in analogy to what is observed in actual nuclei. This is usually attributed to a stronger attraction in n-p pairs compared to pairs of identical particles. The interplay of this quasideuteron effect and usual pairing leads to the ground state quantum numbers of $N = Z$ odd-odd nuclei which satisfy the simple rule $(-)^{J_0+T_0} = -1$ as if the last n-p pair were added to the even-even core with $J_0 T_0 = 0$. The random interaction ensembles give practically the same results.

An analogy to the systems of interacting spins 1/2 (magnetic materials, quantum glasses and quantum computer media) is especially insightful. If the spin-spin interaction for n spins is assumed in a standard form

$$H_s = \sum_{12} \mathcal{J}_{12}(\mathbf{s}_1 \cdot \mathbf{s}_2) \tag{37}$$

with random exchange integrals $\mathcal{J}_{12}$, the ground state spin is also random, increasing in average $\propto \sqrt{n}$ [50]. However, if the system is considered as a specific case of the shell model with many double-degenerate $j = 1/2$ levels, the result is very different: the fraction of $J_0 = 0$ is growing to nearly 100% [51]. In the case (37) the interactions in singlet and triplet states are firmly correlated being determined for each pair by a single exchange integral: the ratio of energies 3:1 is fixed by spin geometry. In the shell model these quantities are uncor-

related. In such a situation, the main contribution comes from the off-diagonal matrix elements as it was mentioned above in relation to the pairing effects. For many levels of $j = 1/2$, the off-diagonal transitions prevail driving the fraction of ground state spins to 1.

Coming back to the question of the reasons determining the ground state quantum numbers in complex nuclei, we need to correct the standard point of view. Certainly, isovector and isoscalar pairing effects push down energies of the states with lowest J and T. However, the geometrical chaoticity plays also an important role that is not properly evaluated in the textbooks.

8 Conclusion

Avoiding an unnecessary repetition, I would like just to stress that ideas of quantum chaos penetrate various domains of nuclear physics. Nuclear symmetries, local spectral statistics, global behavior of level densities, strength functions and damping of collective modes, response to weak perturbations, thermal equilibrium and phase transitions, Fermi-liquid description, even regularities of ground states - all main topics of nuclear research are influenced immensely by ideas of many-body quantum chaos and complexity. From nuclear physics these approaches proliferate to atomic, molecular and condensed matter physics becoming essential for the functioning of solid state microdevices and future quantum computers. A very important area left aside in this review is that of reactions and continuum effects. The most fundamental problems, such as decoherence and interrelation between the classical approximation and the quantum world, cannot be solved without accounting for chaos and complexity. Even for quantum chromodynamics, quantum chaos is an indispensable tool of research and understanding [52].

References

[1] A. Bohr and B. Mottelson, (1969) *Nuclear Structure* vol. 1 (Benjamin, New York).

[2] M.G. Mayer and J.H.D. Jensen, (1955) *Elementary Theory of Nuclear Shell Structure* (Wiley, New York).

[3] A. Bohr, B.R. Mottelson and D. Pines, (1958) *Phys. Rev.* **110** 936.

[4] S.T. Belyaev, (1959) *Kgl. Danske Vid. Selsk. Mat.-fys. Medd.* **31** No. 11.

[5] M. Horoi, B.A. Brown and V. Zelevinsky, (1995) *Phys. Rev. Lett.* **74** 5190.

[6] V.V. Flambaum and F.M. Izrailev, (1997) *Phys. Rev.* **E55** R13 ; (1997) *Phys. Rev.* **E56** 5144 .

[7] F.J. Dyson, (1962) *J. Math. Phys.* **3** 140, 157, 166.

[8] M.L. Mehta, (1990) *Random Matrices* (Academic, New York).

[9] (1965) *Statistical Theories of Spectra: Fluctuations*, (ed. C.E. Porter; Academic Press, New York).

[10] K.K. Mon and J.B. French, (1975) *Ann. Phys.* **95** 90.

[11] A.P. Zuker, (2001) *Phys. Rev.* **C64** 021303.

[12] L. Molinari and V.V. Sokolov, (1989) *J. Phys.* **A22** L999.

[13] I.I. Gurevich and M.I. Pevsner, (1957) *Nucl. Phys.* **2** 575.

[14] I.I. Gurevich, (1939) *Zh. Eksp. Teor. Phys.* **9** 1283.

[15] J.B.French *et al.*, (1987) *Phys. Rev. Lett.* **58** 2400.

[16] V. Zelevinsky, B.A. Brown, N. Frazier, and M. Horoi, (1996) *Phys. Rep.* **276** 315.

[17] J. Rekstad *et al.*, (1993) *Phys. Rev.* **C47** 2621.

[18] V. Zelevinsky, (1993) *Nucl. Phys.* **A555** 109.

[19] G. Kilgus *et al.*, (1987) *Z. Phys.* **A326** 41.

[20] I.C.Percival, (1973) *J. Phys.* **B6** L229.

[21] F.M.Izrailev, (1990) *Phys. Rep.* **196** 299.

[22] R.Aurich and F.Steiner, (1991) *Physica* **D48** 445.

[23] V.V. Sokolov, B.A. Brown, and V. Zelevinsky, (1998) *Phys. Rev.* **58** 56.

[24] P. Cejnar, V. Zelevinsky and V.V. Sokolov, (2001) *Phys. Rev.* **E63** 036127.

[25] V.V. Flambaum, F.M. Izrailev, and G. Casati, (1996) *Phys. Rev.* **E54** 2136.

[26] M.Srednicki, (1994) *Phys. Rev.* **E50** 888.

[27] O.P.Sushkov and V.V.Flambaum, (1982) *Sov. Phys. Usp.* **25** 1.

[28] V.V. Flambaum and V.G. Zelevinsky, (1995) *Phys. Lett.* **B350** 8.

[29] G.V. Danilyan *et al.*, (1977) *JETP Lett.* **26** 186; G.A. Petrov, (1989) *Nucl. Phys.* **A502** 297.

[30] J.Reiter and H.L.Harney, (1990) *Z. Phys.* **A337** 121.

[31] C.A. Bertulani and V.G. Zelevinsky, (1994) *Nucl. Phys.* **A568** 931.

[32] C.H. Lewenkopf and V. Zelevinsky, (1994) *Nucl. Phys.* **A569** 183c.

[33] N. Frazier, B.A. Brown, and V. Zelevinsky, (1996) *Phys. Rev.* **C54** 1665.

[34] M. Horoi, B.A. Brown and V. Zelevinsky, (1994) *Phys. Rev.* **C50** R2274.

[35] M. Horoi, A. Volya, and V. Zelevinsky, (1999) *Phys. Rev. Lett.* **82** 2064.

[36] M. Horoi, B.A. Brown, and V. Zelevinsky, (2002) *Phys. Rev.* **C65** 027303.

[37] C.W. Johnson, G.F. Bertsch, and D.J. Dean, (1998) *Phys. Rev. Lett.* **80** 2749.

[38] C.W. Johnson, G.F. Bertsch, D.J. Dean, and I. Talmi, (2000) *Phys. Rev.* **C61** 014311.

[39] R. Bijker, A. Frank, and S. Pittel, (1999) *Phys. Rev.* **C60** 021302.

[40] Y.M. Zhao and A. Arima, (2001) *Phys. Rev.* **C64** 041301.

[41] R. Bijker and A. Frank, (2000) *Phys. Rev. Lett.* **84** 420; (2000) *Phys. Rev.* **C62** 014303.

[42] D. Kusnezov, (2000) *Phys. Rev. Lett.* **85** 3773.

[43] J.B. French and K.F. Ratcliff, (1971) *Phys. Rev.* **C3** 94.

[44] D. Mulhall, A. Volya and V. Zelevinsky, (2000) *Phys. Rev. Lett.* **85** 4016.

[45] M. Horoi, B.A. Brown and V. Zelevinsky, (2001) *Phys. Rev. Lett.* **87** 06251.

[46] Y.M. Zhao, A. Arima, and N. Yoshinaga, *nucl-th/0112075*.

[47] P.H-T. Chau, A. Frank, N.A. Smirnova, and P. Van Isacker, (2002) *Preprint GANIL P 02 11*.

[48] M. Horoi, A. Volya and V. Zelevinsky, (2002) *Phys. Rev.* **C66** 024319.

[49] J.A. Folk *et al.*, (2001) *Phys. Scripta* **T90** 26.

[50] J. Oitmaa and O.P. Sushkov, (2001) *Phys. Rev. Lett.* **87** 167206.

[51] L. Kaplan, T. Papenbrock and C.W. Johnson, (2001) *Phys. Rev. C* **63** 014307.

[52] J.J.M. Verbaarschot and T. Wettig, (2000) *Ann. Rev. Nucl. Part. Sci.* **50** 343.